Ciattoni *et al.*

Perfect optical solitons: spatial Kerr solitons as exact solutions of Maxwell's equations

Alessandro Ciattoni

Istituto Nazionale per la Fisica della Materia, and Consiglio Nazionale Delle Richerche and Dipartimento di Fisica, Universitá dell'Aquila, 67010 L'Aquila, Italy

Bruno Crosignani

Dipartimento di Fisica, Universitá dell'Aquila, 67010 L'Aquila, Italy, Istituto Nazionale di Fisica della Materia, UdR Roma "La Sapienza," 00185 Roma, Italy, and California Institute of Technology 128-95, Pasadena, California 91125

Paolo Di Porto

Dipartimento di Fisica, Universitá dell'Aquila, 67010, L'Aquila, Italy and Istituto Nazionale di Fisica della Materia, UdR Roma "La Sapienza," 00185 Roma, Italy

Amnon Yariv

California Institute of Technology 128-95, Pasadena, California 91125

We prove that spatial Kerr solitons, usually obtained in the frame of a nonlinear Schrödinger equation valid in the paraxial approximation, can be found in a generalized form as exact solutions of Maxwell's equations. In particular, they are shown to exist, both in the bright and dark version, as TM, linearly polarized, exactly integrable one-dimensional solitons and to reduce to the standard paraxial form in the limit of small intensities. In the two-dimensional case, they are shown to exist as azimuthally polarized, circularly symmetric dark solitons. Both one- and two-dimensional dark solitons exhibit a characteristic signature in that their asymptotic intensity cannot exceed a threshold value in correspondence of which their width reaches a minimum sub-wavelength value. © 2005 Optical Society of America

OCIS codes: 190.0190, 190.3270.

1. INTRODUCTION

The analytic description of spatial Kerr solitons, initiated by the seminal paper of Chiao *et al.*,[1] has been continuously evolving over the past forty years.[2,3] This description basically hinges upon the use of the nonlinear Schrödinger equation (NLS), which in turn follows from the nonlinear Helmholtz equation once the paraxial approximation, limiting the size w of the propagating beam to values large compared with the wavelength λ, is introduced. This approximation becomes inappropriate if the beam size w is comparable with λ, a regime where nonparaxial effects become important and are eventually able to provide a mechanism for avoiding nonphysical behaviors (like, e.g., catastrophic collapse) in the beam evolution. Although many contributions have been produced in this direction,[4–13] they are typically based on some form of asymptotic expansion in the smallness parameter $\eta = \lambda/w$ and are thus limited to the range $\eta < 1$. To overcome this limitation, we start *ab initio* from Maxwell's equations and look for exact soliton solutions. More precisely, we solve Maxwell's equations in the presence of a fully vectorial Kerr polarizability and find a class of rigorous optical solitons that inherently include all nonparaxial contributions. This is separately performed for one-

dimensional and two-dimensional spatial solitons, both in the bright and dark configuration. In particular, the one-dimensional case is dealt with by reducing Maxwell's equations to a system of first-order differential equations and is handled by appealing to the usual formalism employed in the frame of dynamical systems. Our system is shown to posses a first integral, so that its integrability is proved and the boundary value problem, associated with solitons, is solved in closed analytical form.

One of the main results obtained in this paper is the proof of the existence of exact solutions of Maxwell equations in the form of linearly polarized one-dimensional Kerr solitons; they do not suffer of any limitation on the value of w and λ (apart from the obvious one associated with the validity of the macroscopic model of Kerr polarizability), and their existence curve can be numerically evaluated for all values of the beam intensity. Both bright and dark TM solitons can be derived from an integrable system of equations, and their existence curve shows that, in the case of bright solitons, any value of the peak intensity u_{x0}^2 is allowed, while dark solitons can exist only if their asymptotic intensity $u_{x\infty}^2$ does not exceed a threshold value completely determined by the Kerr coefficients. In correspondence to this threshold, their width ap-

proaches the minimum value of the order of a fraction of λ. In the two-dimensional case dark azimuthally polarized solitons are found, and their existence curve implies the same threshold behavior as that of the one-dimensional dark solitons. Although one-dimensional solitons reduce to the standard paraxial ones for small values of the intensity, the two-dimensional azimuthal dark soliton is a completely new entity that has never been studied in the paraxial regime.

We wish to note that the proof of the existence and derivation of exact solitons requires, in the one-dimensional case, the use of a rather sophisticated mathematical analysis borrowed from the dynamical system formalism, which we describe fully in Section 2.

2. ONE-DIMENSIONAL SPATIAL SOLITONS

The electric and magnetic complex amplitudes $\mathbf{E}(\mathbf{r})$ and $\mathbf{B}(\mathbf{r})$ of a monochromatic electromagnetic field $\mathrm{Re}[\mathbf{E} \times \exp(-i\omega t)]$, $\mathrm{Re}[\mathbf{B} \exp(-i\omega t)]$ propagating in a nonlinear medium obey Maxwell's equations

$$\nabla \times \mathbf{E} = i\omega \mathbf{B},$$

$$\nabla \times \mathbf{B} = -i\frac{\omega}{c^2}n_0^2\mathbf{E} - i\omega\mu_0\mathbf{P}_{nl}, \qquad (1)$$

where n_0 is the linear refractive index and $\mathbf{P}_{nl}$ is the nonlinear polarizability. In the case of nonresonant isotropic media, the vectorial Kerr effect is described by the polarizability[14]

$$\mathbf{P}_{nl} = \frac{4}{3}\epsilon_0 n_0 n_2\left[|\mathbf{E}|^2\mathbf{E} + \frac{1}{2}(\mathbf{E}\cdot\mathbf{E})\mathbf{E}^*\right], \qquad (2)$$

and n_2 is the nonlinear refractive index coefficient. After eliminating $\mathbf{B}$ from Eq. (1) and taking advantage of Eq. (2), we get

$$\nabla \times \nabla \times \mathbf{E} = k^2\mathbf{E} + k^2\frac{4}{3}\frac{n_2}{n_0}\left[|\mathbf{E}|^2\mathbf{E} + \frac{1}{2}(\mathbf{E}\cdot\mathbf{E})\mathbf{E}^*\right], \quad (3)$$

where $k = n_0\omega/c$. We now introduce a Cartesian reference frame $Oxyz$ with unit vectors $\hat{\mathbf{e}}_x$, $\hat{\mathbf{e}}_y$, and $\hat{\mathbf{e}}_z$, and look for TM one-dimensional solitons propagating along the z axis, that is for y-independent fields of the form

$$\mathbf{E}(x,y,z) = \exp(i\alpha z)[U_x(x)\hat{\mathbf{e}}_x + iU_z(x)\hat{\mathbf{e}}_z], \qquad (4)$$

where U_x and U_z depend on x alone and α is a real constant. Substituting Eq. (4) into Eq. (3) yields the system of ordinary differential equations

$$\alpha\frac{\mathrm{d}U_z}{\mathrm{d}x} = \left[(\alpha^2 - k^2) - \frac{2k^2n_2}{n_0}\left(U_x^2 + \frac{1}{3}U_z^2\right)\right]U_x,$$

$$\frac{\mathrm{d}^2U_z}{\mathrm{d}x^2} - \alpha\frac{\mathrm{d}U_x}{\mathrm{d}x} = -k^2\left[1 + \frac{2n_2}{n_0}\left(\frac{1}{3}U_x^2 + U_z^2\right)\right]U_z, \qquad (5)$$

whose unknowns U_x and U_z are real [as a consequence of the $\pi/2$ phase difference we introduced between the transverse and longitudinal field components; see Eq. (4)]. Note that the field in Eq. (4) has a vanishing y component,

a requirement not forbidden by Maxwell's equations. From Eqs. (5), it is evident that the z component U_z vanishes only if $U_x = \pm[(n_0/2n_2)(\alpha^2/k^2 - 1)]^{1/2}$, a relation that describes a family of solitary plane waves rather than solitons.[15] The fact that, in general, U_z does not vanish is a consequence of the vectorial coupling between the transverse and the longitudinal components that cannot be rigorously neglected when describing spatially nonuniform fields, like, for example, solitons. Note that the longitudinal component is usually neglected in the paraxial regime owing to the slow variation of the transverse component as compared with the wavelength $\lambda = 2\pi/k$, a circumstance that allows us to treat it as a perturbation for slightly nonparaxial beams.[16,17] In the present paper, we deal on equal footing with both transverse and longitudinal components, and it is their simultaneous nonvanishing and coupling that allow us to find exact solitons.

Equations (5) can be recast in a more symmetric form by differentiating the first one and consequently eliminating $\mathrm{d}^2U_z/\mathrm{d}x^2$ (together with $\mathrm{d}U_z/\mathrm{d}x$) from the second one, thus getting

$$\frac{\mathrm{d}u_x}{\mathrm{d}\xi} = \frac{\left[\beta^2\left(1 - \frac{2}{3}\gamma u_x^2 + 2\gamma u_z^2\right) + \frac{4}{3}\left(\gamma + 2u_x^2 + \frac{2}{3}u_z^2\right)u_x^2\right]}{\beta\left[1 + \gamma\left(6u_x^2 + \frac{2}{3}u_z^2\right)\right]}u_z$$

$$\equiv Q_x(u_x, u_z|\beta),$$

$$\frac{\mathrm{d}u_z}{\mathrm{d}\xi} = \frac{1}{\beta}\left[(\beta^2 - 1) - 2\gamma\left(u_x^2 + \frac{1}{3}u_z^2\right)\right]u_x \equiv Q_z(u_x, u_z|\beta), \qquad (6)$$

where we have introduced the dimensionless variables $\xi = kx$, $\beta = \alpha/k$ and $(u_x, u_z) = (|n_2|/n_0)^{1/2}(U_x, U_z)$, while $\gamma = n_2/|n_2|$ (so that $\gamma = +1$ and $\gamma = -1$ for focusing and defocusing media, respectively). Equations (6) form a system of first-order differential equations describing any electromagnetic field of the form of Eq. (4), and they are equivalent to Maxwell's equation, provided the relation

$$1 + \gamma\left(6u_x^2 + \frac{2}{3}u_z^2\right) \neq 0 \qquad (7)$$

uniformly (i.e., for any ξ) holds. Equations (6) can be conveniently regarded as an autonomous dynamical system (since Q_x and Q_z do not explicitly depend upon ξ), whose solutions, or orbits, are ξ-parameterized curves $\mathbf{u}(\xi) = [u_x(\xi)u_z(\xi)]^T$ [belonging to the phase plane (u_x, u_z)], tangent at each point to the vector field $\mathbf{Q} = (Q_xQ_z)^T$. Solitons are particular orbits that, for suitable values of β, pass through two special points of the phase plane imposed by the boundary conditions pertinent to each soliton kind (boundary value problem).

The most remarkable and general property of the system shown in Eqs. (6) is that it is a conservative system, i.e., it admits a first integral $F(u_x, u_z|\beta)$, defined over the phase plane, satisfying the relation

$$0 = \frac{\mathrm{d}F}{\mathrm{d}\xi} \equiv \frac{\partial F}{\partial u_x}\frac{\mathrm{d}u_x}{\mathrm{d}\xi} + \frac{\partial F}{\partial u_z}\frac{\mathrm{d}u_z}{\mathrm{d}\xi} = \frac{\partial F}{\partial u_x}Q_x + \frac{\partial F}{\partial u_z}Q_z. \qquad (8)$$

In fact, it is straightforward to prove that the function

$$F(u_x, u_z|\beta) = 2u_x^6 + \frac{4}{3}u_x^4 u_z^2 + \frac{2}{9}u_x^2 u_z^4 - \frac{1}{2}\gamma(3\beta^2 - 4)u_x^4$$

$$+ \frac{1}{3}\gamma(2 - \beta^2)u_x^2 u_z^2 + \frac{1}{2}\gamma\beta^2 u_z^4 - \frac{1}{2}(\beta^2 - 1)u_x^2$$

$$+ \frac{1}{2}\beta^2 u_z^2 \tag{9}$$

obeys Eq. (8) whenever Eq. (7) is satisfied. This implies that F is a first integral of the system of Eqs. (6) whenever this system is equivalent to Maxwell's equations. According to Eq. (8), any solution of Eqs. (6) is constrained to move along a single level set

$$F(u_x, u_z|\beta) = F_0. \tag{10}$$

Inverting Eq. (10) furnishes $u_z = u_z(u_x, F_0, \beta)$ which, once inserted into the first part of Eqs. (6), yields a first-order differential equation solvable by quadratures, thus proving the integrability of Eqs. (6). Note that the first integral in Eq. (9) contains only even powers of u_x and u_z, so that any level set of Eq. (10) is invariant under the inversion of the phase plane $(u_x, u_z) \rightarrow -(u_x, u_z)$.

Exploiting the properties of the first integral found above, we are now in a position to solve in a direct way the soliton boundary value problem, that is, to find suitable values of β (if any) for which a solution $u_x(\xi)$, $u_z(\xi)$ of Eqs. (6) satisfies the general boundary conditions

$$\begin{pmatrix} u_x(0) \\ u_z(0) \end{pmatrix} = \begin{pmatrix} u_{x0} \\ u_{z0} \end{pmatrix} \equiv \mathbf{u}_0, \quad \begin{pmatrix} u_x(+\infty) \\ u_z(+\infty) \end{pmatrix} = \begin{pmatrix} u_{x\infty} \\ u_{z\infty} \end{pmatrix} \equiv \mathbf{u}_\infty. \tag{11}$$

where $\mathbf{u}_0$ and $\mathbf{u}_\infty$ are defined by the kind of soliton, bright or dark, we wish to consider. From a geometrical point of view, this implies that the associated integral curve on the phase plane (u_x, u_z) has to pass through the points $\mathbf{u}_0$ and $\mathbf{u}_\infty$, or, using Eq. (10),

$$F(u_{x0}, u_{z0}|\beta) = F_0,$$

$$F(u_{x\infty}, u_{z\infty}|\beta) = F_0. \tag{12}$$

Since $\mathbf{u}_\infty$ has to be reached for $\xi \rightarrow +\infty$, it is obvious that $\mathbf{u}_\infty$ has to be an equilibrium point of Eqs. (6), that is

$$Q_x(u_{x\infty}, u_{z\infty}|\beta) = 0,$$

$$Q_z(u_{x\infty}, u_{z\infty}|\beta) = 0. \tag{13}$$

Equations (12) and (13) in the unknowns β and F_0 are necessary conditions for the soliton existence. They become also sufficient if, once β and F_0 are determined, one is able to prove that the integral curve actually reaches the point $\mathbf{u}_\infty$. Following the outlined procedure, the existence of both bright and dark solitons will be proved and the corresponding existence conditions and propagation constants β will be found.

A. Bright Solitons
Bright solitons are localized nondiffracting beams, that is solutions of Eqs. (6) vanishing for $|\xi| \rightarrow +\infty$, which in turn requires $\mathbf{u}_\infty = 0$. Note that Eqs. (13) are automatically sat-

isfied by this boundary condition, since the origin $(u_x, u_z) = (0,0)$ is always an equilibrium point of Eqs. (6). The second part of Eqs. (12) directly gives $F_0 = 0$, so that the remaining condition we must impose is the first part of Eq. (12), that is

$$F(u_{x0}, u_{z0}|\beta) = 0. \tag{14}$$

To set the boundary condition $\mathbf{u}_0$ we note that, because of the invariance of the level set in Eq. (10) under inversion of the phase plane, a soliton must be associated with an integral curve starting from and ending at the origin and that this curve must be symmetric under either the reflection $u_x \rightarrow -u_x$ or the reflection $u_z \rightarrow -u_z$. Because of these symmetry properties, we have $\mathbf{u}_0 = (0\ u_{z0})^T$ and $\mathbf{u}_0 = (u_{x0}\ 0)^T$ (where T stands for transposed) in the former and in the latter case, respectively. In the first case, Eq. (14) becomes $\beta^2 u_{z0}^2 (\gamma u_{z0}^2 + 1) = 0$, which implies $\beta = 0$, so that soliton propagation is not allowed. We are left to consider the case $\mathbf{u}_0 = (u_{x0}\ 0)^T$, for which Eq. (14) furnishes

$$\beta^2 = \frac{(1 + 2\gamma u_{x0}^2)^2}{1 + 3\gamma u_{x0}^2}. \tag{15}$$

In Appendix A, we prove that bright solitons exist for all the real values of u_{x0} in focusing media ($\gamma = 1$) and that they never exist in defocusing media ($\gamma = -1$) in agreement with the intuitive behavior of Kerr nonlinearity, which tends to focus and defocus the beam in these two cases, respectively. Obviously, the above results about the existence of bright solitons are based on the validity of Eq. (2), which fails either for intensities so large or for soliton widths so small that the nonlinear refractive index saturates. For $\gamma = 1$, Eq. (15) yields

$$\beta = \pm \frac{1 + 2u_{x0}^2}{(1 + 3u_{x0}^2)^{1/2}}, \tag{16}$$

which is the propagation constant of the exact bright solitons [$\pm$ in Eq. (16) describes the two counterpropagating solitons along the z axis].

Substituting Eq. (16) and $F_0 = 0$ into Eq. (10), we obtain the equation for the integral curves on the phase plane corresponding to bright solitons, and these are reported, for some specific values of u_{x0}, in Fig. 1. Note that, for each $|u_{x0}|$, the corresponding level set is a bow-tie-shaped curve encompassing three orbits of Eqs. (6), that is the origin (which is an equilibrium point) and the left and right loops of the bow tie. These last two orbits correspond to a pair of bright solitons, each of which can be obtained from the other after the inversion of the x-axis, $\xi \rightarrow -\xi$ (implying the reflection $u_x \rightarrow -u_x$ also), as expected because of the reflection invariance along any direction exhibited by Kerr nonlinearity. Considering the right half-plane $u_x > 0$ only, we observe that soliton curve $u_x(\xi), u_z(\xi)$ explores the loop starting from the origin (for $\xi = -\infty$), reaching the point $(u_x, u_z) = (u_{x0}, 0)$ (for $\xi = 0$) and ending at the origin (for $\xi = +\infty$). From Eqs. (6) it is evident that the loop is explored counterclockwise and clockwise for $\beta > 0$ and $\beta < 0$, respectively, so that, for counterpropagating solitons [denoted with $(+)$ and $(-)$], we have $u_x^{(+)}(\xi) = u_x^{(-)}(\xi)$ and $u_z^{(+)}(\xi) = -u_z^{(-)}(\xi)$.

Having proved the bright soliton existence and derived the associated propagation constant β, we are now in the position to obtain the soliton shape for any given u_{x0} by numerically solving Eqs. (6) with β given by Eq. (16) and the initial conditions $u_x(0) = u_{x0}$, $u_z(0) = 0$ [the numerical approach being much simpler than integrating the system Eqs. (6) by quadrature]. In Fig. 2, we report the plots of the transverse u_x and longitudinal u_z components of the bright solitons for the same u_{x0} as in Fig. 1. Note that, as expected, the soliton width decreases for increasing u_{x0}, while the longitudinal component u_z increases. In Fig. 3, we report the bright soliton existence curve, relating the FWHM (Δ_{bright}) to $|u_{x0}|$. As $|u_{x0}|$ decreases, the width increases indefinitely; on the other hand, as $|u_{x0}|$ increases, the width decreases monotonically, eventually approaching zero.
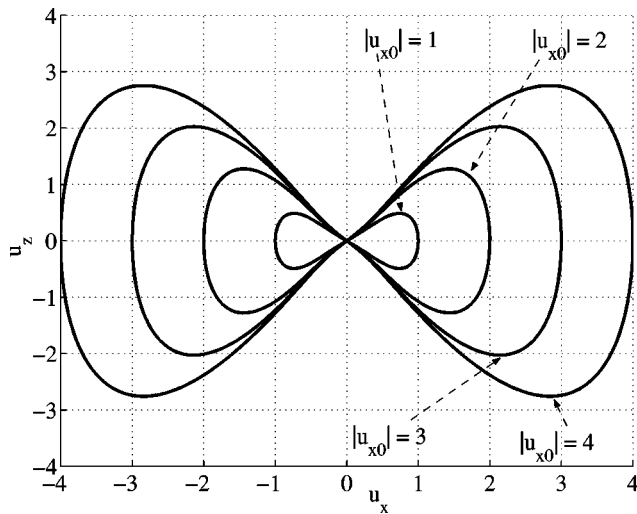

Fig. 1. Plot of phase portrait of Eqs. (6) associated to bright solitons for $|u_{x0}| = 1, 2, 3, 4$. Each bow-tie-shaped curve is obtained by plotting the level set defined in Eq. (14) with β given by Eq. (16). Any piece of curve starting from and ending at the origin (left or right loop of each bow tie) is associated with a single bright soliton.
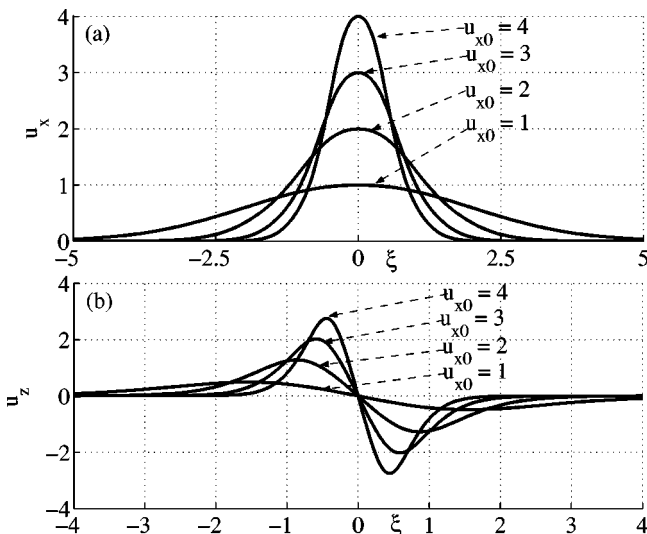

Fig. 2. Plot of (a) the transverse component $u_x(\xi)$ and (b) longitudinal component $u_z(\xi)$ of bright solitons for $u_{x0} = 1, 2, 3, 4$ (same cases as in Fig. 1) and $\beta > 0$.
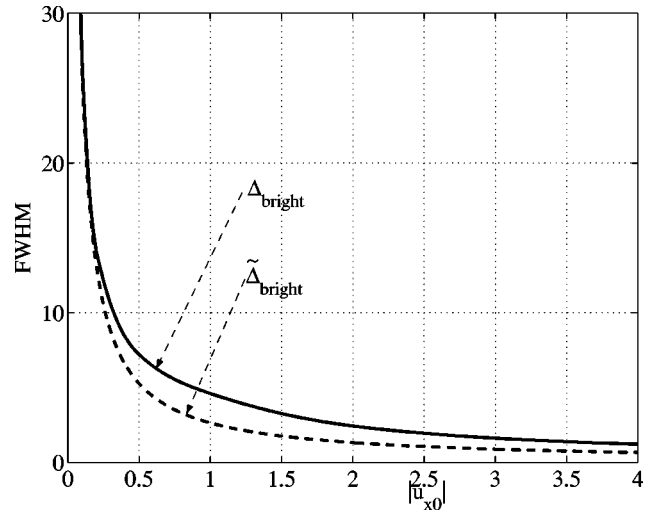

Fig. 3. Bright soliton existence curve (solid curve), relating the FWHM, Δ_{bright}, of the amplitude $u_x(\xi)$ to $|u_{x0}|$. For very small and very large $|u_{x0}|$, the FWHM diverges and vanishes, respectively. The dashed curve represents the FWHM, $\widetilde{\Delta}_{\text{bright}}$, of paraxial bright solitons. Note the complete overlapping of the two curves for $u_{x0} < 0.2$.

B. Dark Solitons

In the scalar approximation, dark solitons are nondiffracting beams vanishing at $\xi = 0$ and approaching an asymptotic amplitude value for $|\xi| \to +\infty$. In our vectorial case, the natural extension of the previous definition is identified with soliton solutions with $\mathbf{u}_0 = (0 \ u_{z0})^T$ and $\mathbf{u}_\infty = (u_{z\infty} \ 0)^T$ [see Eqs. (11)]. In fact, the above boundary conditions will be proved to describe an exact dark soliton that, in the paraxial limit, reduces to the standard scalar dark one.

The chosen values of $\mathbf{u}_\infty$ identically satisfy the first of Eq. (13). The second part of Eqs. (13) implies, with the help of the second of Eqs. (6),

$$\beta^2 = 1 + 2\gamma u_{x\infty}^2. \tag{17}$$

Substituting this value of β^2 together with the boundary conditions into Eqs. (12), we get

$$F_0 = -\frac{\gamma}{2}(1 + 2\gamma u_{x\infty}^2) u_{x\infty}^4,$$

$$u_{x\infty}^4 = -\gamma u_{z0}^2 - u_{z0}^4. \tag{18}$$

The first of these equations furnishes the value F_0 of the first integral along the dark soliton integral curve. The second one is a necessary condition for soliton existence from which we immediately obtain $\gamma = -1$, in agreement with the intuitive property that only defocusing media can support dark solitons. In Appendix B, we prove that dark solitons exist for $u_{x\infty}^2 < 1/6$ only and that

$$\beta = \pm(1 - 2u_{x\infty}^2)^{1/2},$$

$$u_{z0} = \pm\left\{\frac{1}{2}[1 - (1 - 4u_{x\infty}^2)^{1/2}]\right\}^{1/2},$$

$$F_0 = \frac{1}{2}(1 - 2u_{x\infty}^2)u_{x\infty}^4, \tag{19}$$

so that each soliton is completely specified by the value $u_{x\infty}$ only.

As in the case of bright solitons, the integral curves in the phase plane associated with dark solitons are given by Eq. (10), with β and F_0 given in Eqs. (19), few of them being reported in Fig. 4. For each $|u_{x\infty}|$ the level set is a closed curve encompassing four orbits of Eqs. (6), that is, the two equilibrium points $(-u_{x\infty}, 0)$ and $(u_{x\infty}, 0)$ together with the two curves joining these two points in the upper and lower half planes, respectively. These last two orbits are associated with a pair of dark solitons having opposite longitudinal components. Limiting our attention to the upper half-plane $u_z > 0$, the dark soliton curve $u_x(\xi), u_z(\xi)$ starts, for $\beta > 0$, from the point $(-u_{x\infty}, 0)$ at $\xi = -\infty$, reaches the point $(0, u_{z0})$ at $\xi = 0$ and finally ends at the point $(u_{x\infty}, 0)$ at $\xi = +\infty$ (for $\beta < 0$ it is sufficient to invert $\xi \to -\xi$).

For any given value of $u_{x\infty}$ (in the range $|u_{x\infty}| < 1/\sqrt{6}$), the shape of dark solitons can be obtained by numerically integrating Eqs. (6) with β given by the first of Eqs. (19) and initial conditions $u_x(0) = 0$ and $u_z(0) = u_{z0}$ [the latter being given by the second of Eqs. (19)]. In Fig. 5, we plot the transverse u_x and longitudinal u_z components of various dark solitons for the same $u_{x\infty}$ as in Fig. 4. Also in this case, the soliton width decreases for increasing $u_{x\infty}$ while the longitudinal component increases. In Fig. 6 we report the dark soliton existence curve relating the soliton FWHM (Δ_{dark}) to $u_{x\infty}$, in the range $0 < u_{x\infty} < 1/\sqrt{6}$. Note that, for very small $u_{x\infty}$, the FWHM grows indefinitely, whereas in correspondence to the threshold value $u_{x\infty} = 1/\sqrt{6}$, it attains its minimum value $\simeq 4$ corresponding to physical value $\simeq (2/\pi)\lambda \simeq 0.63\lambda$.

C. Optical Intensity

Having derived the electric field [see Eq. (4)] associated with both bright and dark solitons, we can directly evaluate the corresponding magnetic field by means of the per-

Fig. 5. Plot of (a) the transverse component $u_x(\xi)$ and (b) longitudinal component $u_z(\xi)$ of dark solitons for $u_{x\infty} = 0.1, 0.2, 0.3, 0.4$ (same cases as in Fig. 4) and $\beta > 0$.
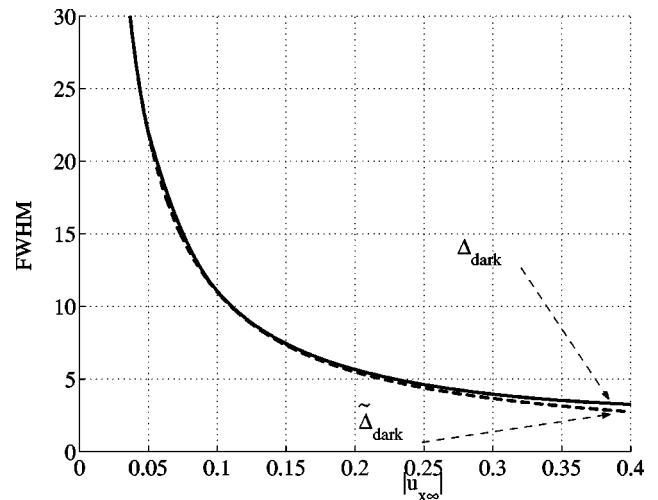
Fig. 6. Dark soliton existence curve (solid curve), relating the FWHM, Δ_{dark} of the amplitude $u_x(\xi)$ to $|u_{x\infty}|$. For very small $|u_{x\infty}|$ the FWHM diverges, whereas at the threshold value $u_{x\infty} = 1/\sqrt{6}$ it attains its minimum value $\simeq 3$. The dashed curve represents the FWHM, $\tilde{\Delta}_{dark}$, of paraxial dark solitons. Note the complete overlap for most of the values of $u_{x\infty}$.

tinent Maxwell equation. Substituting Eq. (4) into the first part of Eqs. (1) we easily deduce

$$\mathbf{B}(x,y,z) = \frac{k}{\omega}\left(\frac{n_0}{|n_2|}\right)^{1/2} \exp(i\beta kz)\left(\beta u_x - \frac{du_z}{d\xi}\right)_{\xi = kx} \hat{\mathbf{e}}_y. \tag{20}$$

Note that the soliton magnetic field is parallel to the y axis and therefore orthogonal to the electric field everywhere, a remarkable vectorial feature that exact solitons share with plane waves (which are, as well, rigorously nondiffracting fields). To describe the soliton energy flow, we can now evaluate the averaged Poynting vector $\mathbf{S} = \text{Re}(\mathbf{E} \times \mathbf{B}^*)/(2\mu_0)$ which, using Eqs. (4) and (20) and the second part of Eqs. (6), turns out to be
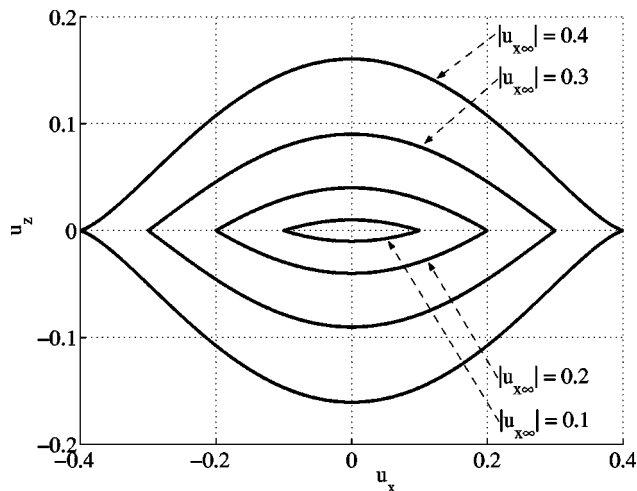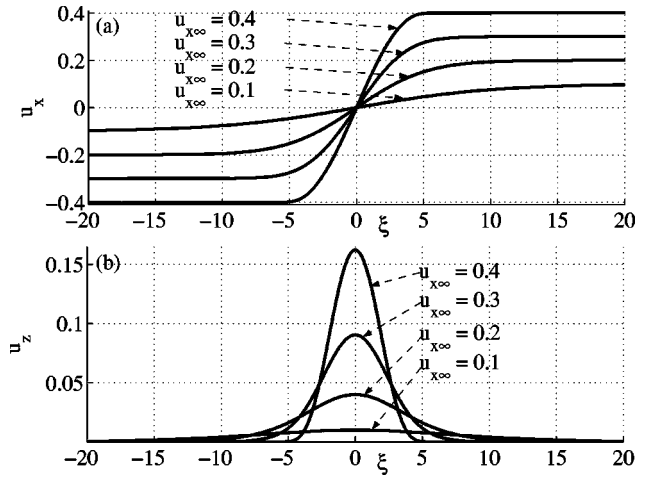
Fig. 4. Plot of phase portrait of Eqs. (6) associated with dark solitons for $|u_{x\infty}| = 0.1, 0.2, 0.3, 0.4$. Each loop is obtained by plotting the level set defined in Eq. (10) with β and F_0 given in Eqs. (19). Any piece of curve joining the points $(-u_{x\infty}, 0)$ and $(u_{x\infty}, 0)$ is associated with a single dark soliton.

$$\mathbf{S} = \frac{I_0}{\beta}\left[1 + 2\gamma\left(u_x^2 + \frac{1}{3}u_z^2\right)\right]u_x^2\hat{\mathbf{e}}_z \equiv \frac{\beta}{|\beta|}I\hat{\mathbf{e}}_z, \qquad (21)$$

where $I_0 = kn_0/(2\omega\mu_0|n_2|)$ and I, the modulus of the averaged Poynting vector, is the optical intensity. The averaged Poynting vector is everywhere parallel to the z axis, and this is fully consistent with the nondiffracting nature of the solitons we are considering. This result (which is not rigorously valid in the paraxial limit) is a necessary consequence of the exact description of any nondiffracting field since a nonvanishing transverse component of the averaged Poynting would imply a lateral emission of energy accompanied by a distortion of the field along the propagation direction. Note that the expression in square brackets of Eq. (21) is always positive [while this is trivial in the case $\gamma = +1$, in the case $\gamma = -1$ all the orbits $u_x(\xi), u_z(\xi)$ of Eqs. (6) lie inside the ellipse defined in Eqs. (7), which is in turn contained within the ellipse $2(u_x^2 + \frac{1}{3}u_z^2) = 1$, so that the expression in square bracket of Eq. (21) is always positive]. This implies, as expected, that, both for bright and dark solitons, the sign of β determines whether $\mathbf{S}$ is parallel or antiparallel to the z axis. In Fig. 7 we report the plots of the normalized optical intensity I/I_0 for the same bright and dark solitons examined in the previous figures. From Eq. (21) we observe that the optical intensity is in general not proportional to the square modulus of the electric field. However, in the paraxial limit where $u_x \ll 1$, $u_z \ll u_x$ and $\beta \simeq 1$, Eq. (21) gives $I = I_0 u_x^2$, reproducing the well-known result typical of paraxial optics. We can also evaluate the maximum soliton optical intensity, that is Eq. (21) at $\xi = 0$ (and $\gamma = +1$) for bright solitons and at $|\xi| = +\infty$ (and $\gamma = -1$) for dark solitons, thus getting

$$I_{\text{bright}} = I_0(1 + 3u_{x0}^2)^{1/2}u_{x0}^2,$$

$$I_{\text{dark}} = I_0(1 - 2u_{x\infty}^2)^{1/2}u_{x\infty}^2. \qquad (22)$$

From these equations we note that $I_{\text{bright}} > I_0 u_{x0}^2$ whereas $I_{\text{dark}} < I_0 u_{x\infty}^2$ so that, in general, bright and dark solitons
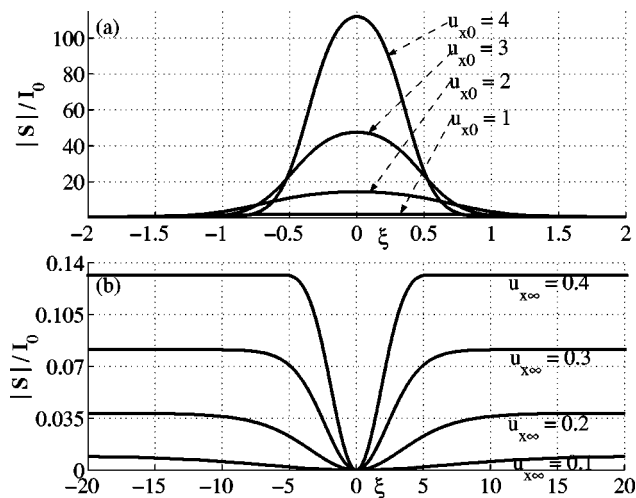

Fig. 7. Normalized optical intensity $|\mathbf{S}(\xi)|/I_0$ of (a) bright and (b) dark solitons evaluated from Eq. (21) for the same soliton conditions as in Fig. 1 (for bright solitons) and Fig. 5 (for dark solitons).

are characterized by an optical intensity that is larger and smaller, respectively, than the corresponding paraxial prediction. This is associated with the fact that, in an extremely narrow soliton, the longitudinal component of the electric field is as large as the transverse one.

D. Paraxial Limit

The above description of one-dimensional bright and dark solitons is exact, with no approximation having been employed in their analytical derivation. As a consequence, the solitons described above are expected to reduce, in the paraxial limit where the soliton width is much larger than the wavelength, to those predicted by the NLS. The paraxial limit is obtained by considering the range of values

$$u_x \ll 1,$$

$$u_z \ll u_x. \qquad (23)$$

In fact the soliton peak intensity is a decreasing function of the width (see Figs. 3 and 6) so that the paraxial limit corresponds to consider small amplitudes [see the first part of Eq. (23)]. Besides, according to the first of Eq. (6), $u_z/u_x \sim (1/u_x)\mathrm{d}u_x/\mathrm{d}\xi$, a quantity much smaller than one in the paraxial approximation [see the second part of Eq. (23)]. By differentiating the first of Eqs. (6), using the second of Eqs. (6) to eliminate $\mathrm{d}u_z/\mathrm{d}\xi$ and exploiting Eqs. (23) to retain only the first relevant order, we obtain

$$\frac{\mathrm{d}^2 u_x}{\mathrm{d}\xi^2} = (\beta^2 - 1)u_x - 2\gamma u_x^3. \qquad (24)$$

Note that, in describing paraxial Kerr solitons, the electric field is usually expressed as $E_x(x,z) = \exp[ik(1+\widetilde{\beta})z] \times (n_0/|n_2|)^{1/2}u_x(\xi)$, where the fundamental plane-wave carrier $\exp(ikz)$ is separated from the slowly varying amplitude of the field. The comparison of this field expression with Eq. (4) yields $\beta = 1 + \widetilde{\beta}$ which, consistently with the paraxial picture where the main plane-wave carrier is slowly modulated ($\widetilde{\beta} \ll 1$), implies $\beta^2 - 1 \simeq 2\widetilde{\beta}$. Introducing this relation into Eq. (24), we get

$$-\widetilde{\beta}u_x + \frac{1}{2}\frac{\mathrm{d}^2 u_x}{\mathrm{d}\xi^2} = -\gamma u_x^3, \qquad (25)$$

which coincides with the usual equation (obtained from the NLS) describing paraxial Kerr solitons. Equation (25) admits both bright soliton solutions ($\gamma = +1$) of the form $u_x(\xi) = u_{x0}\,\mathrm{sech}(u_{x0}\xi)$ and dark soliton solutions ($\gamma = -1$) of the form $u_x(\xi) = u_{x\infty}\tanh(u_{x\infty}\xi)$. The propagation constants are respectively given by $\widetilde{\beta} = u_{x0}^2/2$ and $\widetilde{\beta} = -u_{x\infty}^2$, which can also be found, *mutatis mutandis*, from Eqs. (16) and the first part of Eqs. (19), whenever the paraxial conditions ($u_{x0} \ll 1$ for bright solitons and $u_{x\infty} \ll 1$ for dark solitons) are satisfied. These solitons obviously coincide with the asymptotic paraxial limit of the solitons described in this paper. To make this comparison more quantitative, in Fig. 3 and Fig. 6 we have superimposed on the exact soliton existence curves (solid curves) their paraxial counterparts (dashed curves). More precisely, the FWHM of bright and dark paraxial solitons are easily shown to be $\widetilde{\Delta}_{\text{bright}}$

$=2.6348/u_{x0}$ and $\widetilde{\Delta}_{\text{dark}}=1.0986/u_{x\infty}$. As expected, the paraxial and exact curves are practically indistinguishable for small u_{x0} or $u_{x\infty}$. Not surprisingly, for dark solitons, the agreement between exact and paraxial prediction is satisfactory almost everywhere, since the value of $u_{x\infty}$ is restricted to be less than $1/\sqrt{6}$ corresponding to a moderate nonparaxial regime.

E. Modulational Instability

The solitons we are considering are completely new entities (even if in the paraxial limit they coincide with NLS solitons), so that an analysis of modulational stability is in order since it dictates their feasibility. To this end, we note that Eq. (3) (equivalent to Maxwell's equations) admits the simplest solution in the form of a continuous wave given by

$$E_x(x,z) = V_x \exp\left[ik\Gamma\left(-\frac{V_z}{V_x}x+z\right)\right],$$

$$E_z(x,z) = V_z \exp\left[ik\Gamma\left(-\frac{V_z}{V_x}x+z\right)\right], \qquad (26)$$

where V_x and V_z are two real constants and

$$\Gamma = \left[\frac{1 + \gamma\dfrac{2|n_2|}{n_0}(V_x^2 + V_z^2)}{1 + \dfrac{V_z^2}{V_x^2}}\right]^{1/2}. \qquad (27)$$

While in focusing media ($\gamma=+1$) these continuous waves exist for any choice of the amplitudes V_x and V_z, since Γ is always real; in defocusing media ($\gamma=-1$) the reality of Γ implies that continuous waves exist if the relation $V_x^2 + V_z^2 < n_0/(2|n_2|)$ is satisfied. To investigate the linear stability of the exact solutions provided by Eqs. (26) against small perturbation, we look for solutions of Eq. (3) describing small variations around the exact solution, in the form

$$E_x(x,z) = [V_x + v_x(x,z)]\exp\left[ik\Gamma\left(-\frac{V_z}{V_x}x+z\right)\right],$$

$$E_z(x,z) = [V_z + v_z(x,z)]\exp\left[ik\Gamma\left(-\frac{V_z}{V_x}x+z\right)\right], \qquad (28)$$

where the moduli of the complex fields v_x and v_z are assumed to be small. Inserting Eqs. (28) into Eq. (3) we obtain, after linearization, a system of two linear equations for v_x and v_z that are equivalent to four linear equations for their real and imaginary parts. Looking for eigensolutions of the form $\text{Re}(v_x), \text{Im}(v_x), \text{Re}(v_z), \text{Im}(v_z) \propto \exp[ik(Q_x x + Q_z z)]$ and considering only continuous waves with $V_z = 0$ (in order to simplify the mathematical treatment), we obtain the dispersion relation
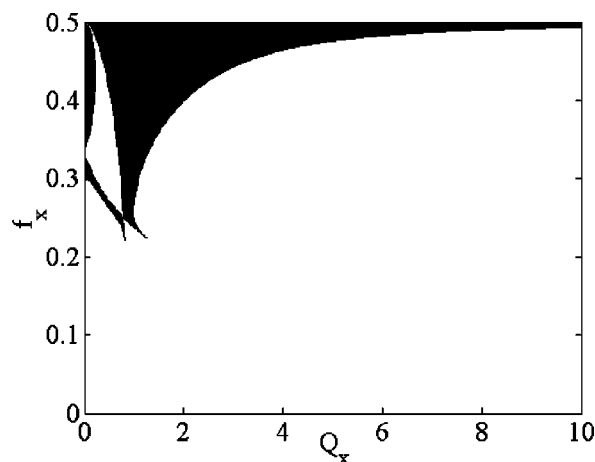

Fig. 8. Values of $f_x = (|n_2|/n_0)^{1/2}V_x$ and Q_x (black region), where no modulational instability is present in defocusing ($\gamma=-1$) media.

$$-3\Gamma^2(2-3\Gamma^2)Q_x^4 + \Gamma^2(2+\Gamma^2)Q_z^4 + 2(3\Gamma^4 + 2\Gamma^2 - 2)Q_x^2 Q_z^2$$
$$+ 2\Gamma^2(1-\Gamma^2)(2+\Gamma^2)Q_x^2 - 2\Gamma^2(3\Gamma^4 + 5\Gamma^2 - 2)Q_z^2 = 0$$

$$(29)$$

relating the dimensionless wave vector (Q_x, Q_z) of the perturbation to the normalized amplitude $f_x = (|n_2|/n_0)^{1/2}V_x$ of the continuous wave through the coefficient $\Gamma = (1 + 2\gamma f_x^2)^{1/2}$. Equation (29) furnishes four values of $Q_z(Q_x, f_x)$ so that the perturbation is unstable at the values of Q_x and f_x for which $\text{Im}(Q_z) \neq 0$. It is possible to find analytically the four roots of Eq. (29), since it is biquadratic in Q_z. These roots turn out to be rather complicated and, for simplicity, we report here only the main results. In focusing media ($\gamma=1$) the four values of $Q_z(Q_x, f_x)$ turn out to all have a nonvanishing imaginary part for any (Q_x, f_x), so that perturbations are always unstable. This is related to the feasibility (and hence the existence) of bright solitons in focusing media, since a spatially localized solution (with vanishing asymptotics) cannot be observed if the plane-wave solution is stable. The case of defocusing media ($\gamma=-1$) is a little more involved. In Fig. 8, we report the region (in black) of the plane (Q_x, f_x) where the imaginary parts of all the solutions $Q_z(Q_x, f_x)$ of Eq. (29) are vanishing, i.e., the region where continuous plane waves are stable. The existence of such a region in defocusing media shows that stable plane-wave solutions do not exist, which is in turn related to the observability of dark solitons; in fact, they can exist only if the continuous plane wave does not break up into a multiplicity of distinct beams.

3. TWO-DIMENSIONAL CASE: AZIMUTHALLY POLARIZED SPATIAL DARK SOLITONS

To deal with the two-dimensional case, we introduce polar cylindrical coordinates r, φ, z with unit vectors $\hat{\mathbf{e}}_r, \hat{\mathbf{e}}_\varphi, \hat{\mathbf{e}}_z$ and look for fields of the form

$$\mathbf{E}(r,\varphi,z) = E_\varphi(r,z)\hat{\mathbf{e}}_\varphi + E_z(r,z)\hat{\mathbf{e}}_z, \qquad (30)$$

describing a circularly symmetric configuration with vanishing radial component. Inserting Eq. (30) into Eq. (3), we obtain

$$\frac{\partial^2 E_z}{\partial r \partial z} = 0,$$

$$\frac{\partial^2 E_\varphi}{\partial z^2} + \frac{\partial}{\partial z}\left(\frac{\partial E_\varphi}{\partial r} + \frac{E_\varphi}{r}\right) = -k^2 E_\varphi - k^2 \frac{4}{3}\frac{n_2}{n_0}$$

$$\times\left[|\mathbf{E}|^2 E_\varphi + \frac{1}{2}(\mathbf{E} \cdot \mathbf{E})E_\varphi^*\right],$$

$$\frac{\partial^2 E_z}{\partial r^2} + \frac{1}{r}\frac{\partial E_z}{\partial r} = -k^2 E_z - k^2 \frac{4}{3}\frac{n_2}{n_0}\left[|\mathbf{E}|^2 E_z + \frac{1}{2}(\mathbf{E} \cdot \mathbf{E})E_z^*\right].$$

$$(31)$$

Internal consistency of the set of Eqs. (31) (three equations in two unknowns) requires $E_z = 0$. As a consequence, the second of Eqs. (31) yields

$$\frac{\partial^2 E_\varphi}{\partial z^2} + \frac{\partial}{\partial r}\left(\frac{\partial E_\varphi}{\partial r} + \frac{E_\varphi}{r}\right) = -k^2 E_\varphi - 2k^2 \frac{n_2}{n_0}|E_\varphi|^2 E_\varphi. \quad (32)$$

We note that circular symmetry and polarization imposed on the field, together with the symmetry properties of Kerr effect, have allowed us to reduce Maxwell's equations to the single Eq. (32). Equation (32) is conveniently rewritten in the dimensionless form

$$\frac{\partial^2 U}{\partial \zeta^2} + 2\frac{\partial}{\partial \rho}\left(\frac{\partial U}{\partial \rho} + \frac{U}{\rho}\right) = -U - 2\gamma|U|^2 U, \quad (33)$$

where $\rho = \sqrt{2}kr$, $\zeta = kz$, $U = (|n_2|/n_0)^{1/2}E_\varphi$ and $\gamma = n_2/|n_2|$. If we look for soliton solutions of the form

$$U(\rho,\zeta) = \exp(i\alpha\zeta)u(\rho), \quad (34)$$

Eq. (33) becomes

$$\frac{\mathrm{d}}{\mathrm{d}\rho}\left(\frac{\mathrm{d}u}{\mathrm{d}\rho} + \frac{u}{\rho}\right) = \frac{1}{2}(\alpha^2 - 1)u - \gamma u^3. \quad (35)$$

Both the structure of Eq. (35) and the azimuthal field polarization dictate $u(0) = 0$, so azimuthally polarized bright solitons do not exist. To find dark solitons, we introduce the further condition

$$\lim_{\rho \to \infty} u(\rho) = u_\infty, \quad (36)$$

together with the vanishing of all derivatives for $\rho \to \infty$. Since focusing media ($\gamma = 1$, i.e., $n_2 > 0$) are not able to support dark solitons, we consider hereafter defocusing media ($\gamma = -1$, i.e., $n_2 < 0$), so that Eq. (35) reads

$$\frac{\mathrm{d}}{\mathrm{d}\rho}\left(\frac{\mathrm{d}u}{\mathrm{d}\rho} + \frac{u}{\rho}\right) = \frac{1}{2}(\alpha^2 - 1)u + u^3, \quad (37)$$

which implies, in view of the above boundary condition at infinity,

$$\alpha = \pm(1 - 2u_\infty^2)^{1/2}. \quad (38)$$

Although positive and negative signs of α respectively refer to forward and backward traveling solitons [see Eq. (34)], $u(\rho)$ depends on α^2 [see Eq. (35)]. Equation (38)

shows the existence of an upper threshold for the soliton asymptotic amplitude

$$u_\infty < \frac{1}{\sqrt{2}}, \quad (39)$$

since, otherwise, α would become imaginary. If we now insert Eq. (38) into Eq. (37), we obtain

$$\frac{\mathrm{d}}{\mathrm{d}\rho}\left(\frac{\mathrm{d}u}{\mathrm{d}\rho} + \frac{u}{\rho}\right) = (u^2 - u_\infty^2)u. \quad (40)$$

We have carried out a numerical integration of Eq. (40) with boundary conditions $u(0) = 0$ and $u(\infty) = u_\infty$ by employing a standard shooting-relaxation method for boundary value problems. Our simulations show that dark solitons can be obtained in the range of field amplitudes $0 < u_\infty < 1/\sqrt{2}$. Different soliton profiles are shown in Fig. 9.

We complete our analysis evaluating both the magnetic field and the Poynting vector. Recalling the expression of the soliton electric field

$$\mathbf{E} = \left(\frac{n_0}{|n_2|}\right)^{1/2} \exp(i\alpha kz)u(\sqrt{2}kr)\hat{\mathbf{e}}_\varphi, \quad (41)$$

we obtain, from the first part of Eqs. (1) written in cylindrical coordinates,

$$\mathbf{B} = -\left(\frac{n_0}{|n_2|}\right)^{1/2} \exp(i\alpha kz)\frac{k}{\omega}\left[\alpha u \hat{\mathbf{e}}_r + i\sqrt{2}\left(\frac{\mathrm{d}u}{\mathrm{d}\rho} + \frac{u}{\rho}\right)\hat{\mathbf{e}}_z\right]_{\rho=\sqrt{2}kr}.$$

$$(42)$$

The magnetic field has a radial component whose shape coincides with that of the electric field and a vanishing azimuthal component, so that $\mathbf{E}$ and $\mathbf{B}$ are mutually orthogonal. With the help of Eqs. (41) and (42), the time-averaged Poynting vector
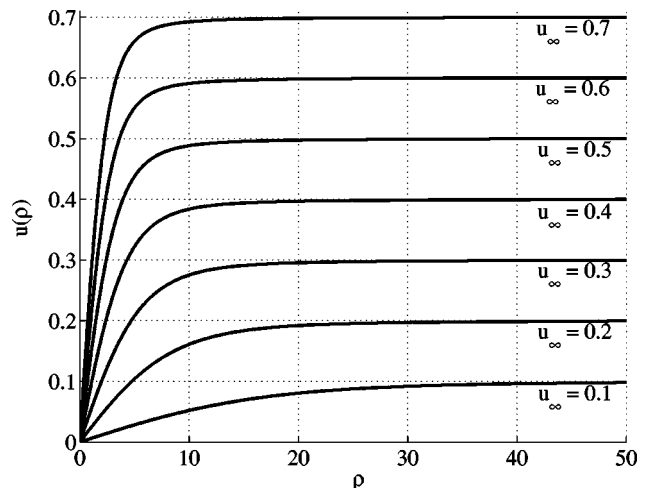

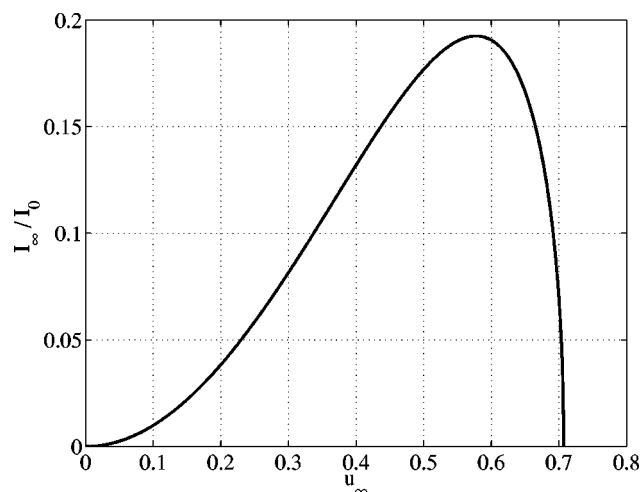Fig. 9. Two-dimensional dark soliton profile $u(\rho)$ for various values of u_∞.

Fig. 10.   Normalized asymptotic optical intensity I_∞/I_0 as a function of the asymptotic dimensionless field amplitude u_∞. Note that two solitons exist for any allowed asymptotic optical intensity.

$$\mathbf{S} = \frac{1}{2\mu_0} \operatorname{Re}(\mathbf{E} \times \mathbf{B}^*) \qquad (43)$$

turns out to be given by

$$\mathbf{S}(r) = \frac{\alpha k}{2\omega\mu_0} \frac{n_0}{|n_2|} u^2(\sqrt{2}kr)\hat{\mathbf{e}}_z = \frac{\alpha k}{2\omega\mu_0}|\mathbf{E}|^2\hat{\mathbf{e}}_z. \qquad (44)$$

We note that $\mathbf{S}$ is parallel to the z axis, consistent with the shape-invariant nature of solitons. From an analytical point of view, this corresponds to the $\pi/2$ phase difference between B_z and E_φ [see Eqs. (41) and (42)]. As expected, the Poynting vector is either parallel or antiparallel to $\hat{\mathbf{e}}_z$ according to the sign of α, while its amplitude is proportional to $|\mathbf{E}|^2$. The above plane-wave-like properties are consistent with the nondiffractive nature of exact solitons.

It is worthwhile to underline that, in the case of the azimuthal dark solitons we are considering, the asymptotic optical intensity $I_\infty = |\mathbf{S}(\infty)|$ turns out to be not proportional to u_∞^2. In fact, by using Eqs. (38) and (44), one obtains

$$I_\infty(u_\infty) = I_0 u_\infty^2 (1 - 2u_\infty^2)^{1/2}, \qquad (45)$$

where $I_0 = kn_0/(2\omega\mu_0|n_2|)$, whose profile is reported in Fig. 10. Equation (45) shows that the asymptotic optical intensity is not a monotonically increasing function of the asymptotic field amplitude but reaches its maximum threshold value $I_\infty^{\max} = I_0/3^{3/2}$ in correspondence to $u_\infty = 1/\sqrt{3}$. This is connected to the α dependence of the magnetic field [see Eq. (42)] whose radial part tends to vanish for $u_\infty \to 1/\sqrt{2}$. A related and relevant consequence of Eq. (45) is the existence of two solitons of different widths for a given asymptotic optical intensity. The existence curve relating the normalized half width at half maximum (HWHM) of the soliton optical intensity profile $|\mathbf{S}(\rho)|$ to u_∞ is reported in Fig. 11. In particular, Fig. 11 shows the existence of a normalized minimum HWHM $\simeq 2.1$ ($\simeq 0.24\lambda$) for $u_\infty = 1/\sqrt{2}$. In addition, Fig. 10 shows that a normalized HWHM $\simeq 2.7$ ($\simeq 0.3\lambda$) corresponds to $u_\infty = 1/\sqrt{3}$, for which

the soliton attains the maximum asymptotic optical intensity $I_\infty^{\max}$.

It is interesting to examine the behavior of our solution in the limit of large ρ. To this end, neglecting in Eq. (40) the term in u/ρ, we obtain

$$\frac{\mathrm{d}^2 u}{\mathrm{d}\rho^2} = (u^2 - u_\infty^2)u, \qquad (46)$$

which formally coincides with the equation describing one-dimensional linearly polarized paraxial dark solitons. Equation (46) admits the solution $u = u_\infty \tanh(\rho u_\infty/\sqrt{2})$. This solution can be compared with the exact one. This is done in Fig. 12, where the ratio $R(\rho)$ between the hyperbolic tangent and the exact solution is showed as a function of ρ, for different values of u_∞. The hyperbolic tangent solution reproduces the exact one for large values of ρ, as expected, while it at most differs by a factor $\cong 1.2$ for small values of ρ.

Finally, we wish to note that, for large values of $|u|^2$, other nonlinear contributions may become significant
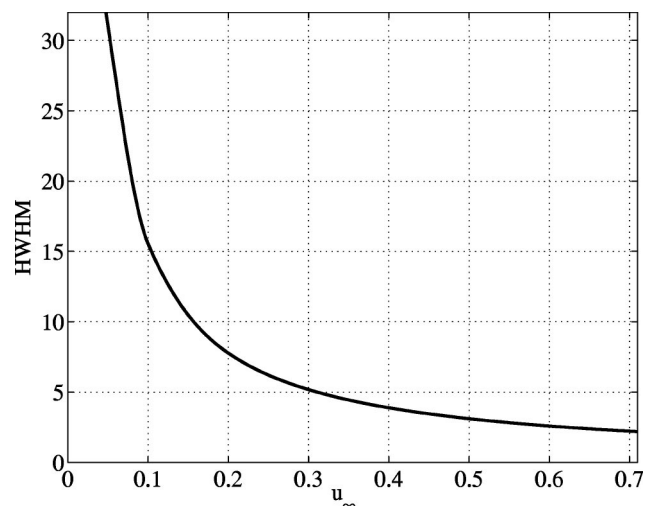

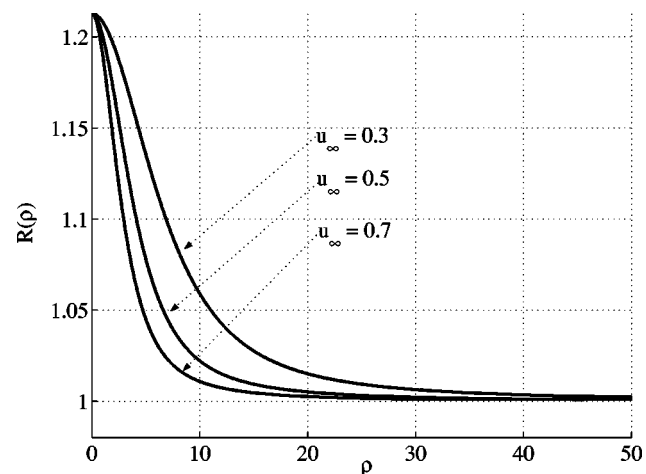Fig. 11.   Existence curve relating the normalized soliton optical intensity HWHM to u_∞.

Fig. 12.   Plot of the ratio $R(\rho) = u_\infty \tanh(u_\infty\rho/\sqrt{2})/u(\rho)$ for different values of u_∞.

enough to affect the validity of Eq. (2). However, in our case, $|u|^2$ is limited by the upper value 1/2 [see Eq. (39)] and these contributions are likely to be negligible. As an example, we can compare the standard cubic term $|u|^2 u$ with the quintic one, which can be written as $(1/2)\kappa^2|u|^4 u$ (see Ref. 18), where $\kappa=1/(kw)$ (k and w being the wave number and the beam width). The quintic term is obviously negligible when $(1/2)\kappa^2|u_\infty|^2\ll 1$, i.e., assuming $w \simeq \lambda/4$, for $|u_\infty|^2\ll 5$.

4. CONCLUSIONS

In this paper, the problem of the existence of nonparaxial spatial Kerr solitons has been solved rigorously. This has been done by showing that spatial solitons can be derived as exact solutions of Maxwell equations (thus making, within our approach, the terms "paraxial" and "nonparaxial" redundant). In the one-dimensional case, our exact optical soliton represents the straightforward generalization of the paraxial one, the main difference being that dark solitons exhibit, unlike their paraxial counterparts, a specific upper limit for the possible values that their asymptotic intensity can assume. In the two-dimensional case, the exact dark soliton is of a completely new kind, and the difference between paraxial and nonparaxial becomes rather meaningless. In any case, the comparison between paraxial and exact solitons done, for example, by inspecting the relative existence curves, shows that our solitons are a definite entity, independent of any approximation scheme; the transition between the paraxial and the highly diffractive regime is very smooth and does not exhibit any kind of dramatic catastrophic behavior, as implied by the standard paraxial theory.

Finally, we note that many attempts have been made in the past few years to deal with fully nonparaxial spatial solitons, both in the unsaturated[19–22] and in the saturated,[18,23,24] nonlinear regime. In particular, TM solitons have been considered in Refs. 19–21, where predictions have been made about the fundamental limitation on the FWHM of bright and dark solitons, that is, the minimum width they can achieve ($\lambda/2$ and $\lambda/4$, respectively). However, none of the above approaches deals with the analytic integrability of Maxwell's equations (which is the main contribution of our paper) and, besides, they all rely on a scalar approximated description of the nonlinear response of the medium. Our description of unsaturated Kerr nonlinearity, on the contrary, is fully tensorial [see Eq. (2)] and thus includes all possible vectorial effects. Consequently, their prediction about the minimum width of the bright solitons is not correct; indeed, our exact approach predicts that the width of the bright soliton can approach zero for increasing intensities (see, e.g., Fig. 3). In Ref. 23 a saturable nonlinear model is adopted that is apt to deal with the very high intensity regime, and the associated numerical solution can be compared with our analytic description only when the intensities are such that the purely cubic nonlinear model is correct. In particular, in the two-dimensional case we describe a new kind of azimuthally polarized dark solitons and show that they exist only if their asymptotic intensity does not exceed a threshold value that turns out to be such that saturation effects are not relevant.

APPENDIX A: EXISTENCE OF BRIGHT SOLITONS IN FOCUSING MEDIA

To tackle the problem of the existence of bright solitons we have to prove that the curve defined in Eq. (14), with β^2 given by Eq. (15), actually reaches the origin of the phase plane (u_x, u_z). To this end, it is convenient to introduce the polar coordinate defined by $u_x=\rho\cos\phi$ and $u_z=\rho\sin\phi$, so that Eq. (14) becomes

$$\rho^2\left\{\rho^4\cos^2\phi\left[2\cos^2\phi+\frac{4}{3}\cos^2\phi\sin^2\phi+\frac{2}{9}\sin^4\phi\right]\right.$$
$$+\gamma\rho^2\left[\frac{1}{2}(4-3\beta^2)\cos^4\phi+\frac{1}{3}(2-\beta^2)\cos^2\phi\sin^2\phi\right.$$
$$\left.+\frac{1}{2}\beta^2\sin^4\phi\right]+\frac{1}{2}[(1-\beta^2)\cos^2\phi+\beta^2\sin^2\phi]\left.\right\}=0.$$

$$(47)$$

This equation is trivially satisfied by setting $\rho=0$, and this is consistent with the fact that the origin is in itself an orbit of Eqs. (6). Therefore the integral curve associated with solitons is described by the vanishing of the expression within the curly brackets. Requiring that this curve reaches the origin yields

$$\tan^2\phi_0=1-\frac{1}{\beta^2}\equiv u_{0x}^2\frac{4u_{0x}^2+\gamma}{(1+2\gamma u_{x0}^2)^2}, \qquad (48)$$

where $\phi_0=\phi(\rho=0)$ and β^2 has been obtained from Eq. (15). For $\gamma=1$, the right-hand side of Eq. (48) is positive, so this equation can always be solved, together with the fact that Eq. (7) is always satisfied for $\gamma=1$, implying that bright soliton exists in focusing media for any value of u_{0x}. In the case $\gamma=-1$, the right-hand side of Eq. (48) is positive for $|u_{0x}|>1/2$, so the curve actually reaches the origin. However, in this case, the curve joining the points $(u_x, u_z)=(0,0)$ and $(u_x, u_z)=(u_{x0}, 0)$ unavoidably crosses the ellipse $6u_x^2+(2/3)u_z^2=1$, since its semiaxis along the x axis is $1/\sqrt{6}<1/2$. Therefore, for $\gamma=-1$, a point belonging to the integral curve such that Eq. (7) fails to be satisfied always exists, with the consequence that, in defocusing media, bright solitons never exist.

APPENDIX B: CONDITIONS FOR THE EXISTENCE OF DARK SOLITONS

As already explained in Section 2, Eqs. (17) and (18) are necessary for the existence of dark solitons, so we have to find when they are also sufficient. From Eq. (17) (with $\gamma=-1$) it is evident that solitons can exist for $u_{x\infty}^2<1/2$. The equation for the dark soliton integral curve on the phase plane [Eq. (10), with β and F_0 given in Eqs. (19)] can be solved for u_z^2 thus yielding

$$u_z^2 = -\frac{\frac{8}{3}u_x^4 - \frac{2}{3}(1 + 2u_{x\infty}^2)u_x^2 + (1 - 2u_{x\infty}^2)}{\frac{8}{9}u_x^2 - 2(1 - u_{x\infty}^2)} + \left\{\left[\frac{8}{3}u_x^4 - \frac{2}{3}(1 + 2u_{x\infty}^2)u_x^2 + (1 - 2u_{x\infty}^2)\right]^2 - \left[\frac{16}{9}u_x^2 - 4(1 - 2u_{x\infty}^2)\right]\right.$$

$$\left. \times [4u_x^6 - (1 + 6u_{x\infty}^2)u_x^4 + 2u_{x\infty}^2 u_x^2 - (1 - 2u_{x\infty}^2)u_{x\infty}^4]\right\}^{1/2} \bigg/ \left[\frac{8}{9}u_x^2 - 2(1 - 2u_{x\infty}^2)\right], \tag{49}$$

which furnishes u_z^2 as a function of u_x^2 (parametrically dependent on $u_{x\infty}^2$) along the dark soliton integral curve. Here, the plus sign between the two terms has been chosen in order to satisfy the boundary condition $u_z(u_{x\infty}^2) = 0$. Evaluating Eq. (49) at $u_x = 0$ and taking the square root of the result, we obtain the second of Eqs. (19), which is consistent with the boundary conditions since it satisfies the second part of Eqs. (18) (with $\gamma = -1$). Therefore, in order to prove soliton existence, we are left with proving that the curves in Eq. (49) actually reach the point $\mathbf{u}_\infty = (u_{x\infty}\ 0)^T$ [i.e., that the right-hand side of Eq. (49) is a positive real number] and that such curves do not cross the ellipse $6u_x^2 + (2/3)u_z^2 = 1$, thus leaving Eq. (7) satisfied. Since the expression raised to the 1/2 power is always positive for $u_{x\infty}^2 < 1/2$, we have only to ensure that the right-hand side of Eq. (49) is positive. It is not difficult to show that this is the case whenever

$$4u_x^6 - (1 + 6u_{x\infty}^2)u_x^4 + 2u_{x\infty}^2 u_x^2 - (1 - 2u_{x\infty}^2)u_{x\infty}^4 < 0. \tag{50}$$

Imposing that the maximum of the polynomial in the left-hand side of this inequality is negative, we obtain the condition $u_{x\infty}^2 < 1/6$. The existence of dark solitons in this range for $u_{x\infty}^2$ is finally proved by noting that any integral curve associated with these solitons globally lies within the ellipse $6u_x^2 + (2/3)u_z^2 = 1$, so Eq. (7) is always satisfied.

ACKNOWLEDGMENTS

Alessandro Ciattoni, the corresponding author, can be reached by e-mail at alessandro.ciattoni@aquila.infn.it.

REFERENCES

1. R. Y. Chiao, E. Garmire, and C. H. Townes, "Self-trapping of optical beams," Phys. Rev. Lett. **13**, 479–482 (1964).
2. S. Trillo and W. Torruellas, *Spatial Solitons* (Springer, 2001).
3. Y. Kivshar and G. P. Agrawal, *Optical Solitons: from Fibers to Photonic Crystals* (Academic, 2003).
4. M. D. Feit and J. A. Fleck, Jr., "Beam nonparaxiality, filament formation, and beam breakup in the self-focusing of optical beams," J. Opt. Soc. Am. B **5**, 633–640 (1998).
5. N. Akhmediev, A. Ankiewicz, and J. M. Soto-Crespo, "Does the nonlinear Schrödinger equation correctly describe beam propagation?," Opt. Lett. **15**, 411–413 (1993).
6. G. Fibich, "Small beam nonparaxiality arrests self-focusing of optical beams," Phys. Rev. Lett. **76**, 4356–4359 (1996).
7. A. P. Sheppard and M. Haelterman, "Nonparaxiality stabilizes three-dimensional soliton beams in Kerr media," Opt. Lett. **23**, 1820–1822 (1998).
8. S. Chi and Q. Guo, "Vector theory of self-focusing of an optical beam in Kerr media," Opt. Lett. **20**, 1598–1600 (1995).
9. G. Fibich and B. Ilan, "Vectorial and random effects in self-focusing and in multiple filamentation," Physica D **157**, 112–146 (2001).
10. A. Ciattoni, C. Conti, E. DelRe, P. Di Porto, B. Crosignani, and A. Yariv, "Polarization and energy dynamics in ultrafocused optical Kerr propagation," Opt. Lett. **27**, 734–736 (2002).
11. P. Kelly, "Self-focusing of optical beams," Phys. Rev. Lett. **15**, 1005–1508 (1965).
12. Y. Silberberg, "Collapse of optical pulses," Opt. Lett. **15**, 1282–1284 (1990).
13. G. Fibich and A. L. Gaeta, "Critical power for self-focusing in bulk media and in hollow waveguides," Opt. Lett. **25**, 335–337 (2000).
14. B. Crosignani, A. Cutolo, and P. Di Porto, "Coupled-mode theory of nonlinear propagation in multimode and single-mode fibers: envelope solitons and self-confinement," J. Opt. Soc. Am. **72**, 1136–1144 (1982).
15. Y. Chen and J. Atai, "Maxwell's equations and the vector nonlinear Schrödinger equation," Phys. Rev. E **55**, 3652–3657 (1997).
16. B. Crosignani, A. Yariv, and S. Mookherjea, "Nonparaxial spatial solitons and propagation-invariant pattern solutions in optical Kerr media," Opt. Lett. **29**, 1254–1256 (2004).
17. A. Ciattoni, B. Crosignani, A. Yariv, and S. Mookherjea, "Nonparaxial dark solitons in optical Kerr media," Opt. Lett. **30**, 516–518 (2005).
18. S. Blair, "Nonparaxial one-dimensional spatial solitons," Chaos **10**, 570–583 (2000).
19. A. W. Snyder, D. J. Mitchell, and Y. Chen, "Spatial solitons of Maxwell's equations," Opt. Lett. **19**, 524–526 (1994).
20. E. Granot, S. Sternklar, Y. Isbi, B. Malomed, and A. Lewis, "Subwavelength spatial solitons," Opt. Lett. **22**, 1290–1292 (1997).
21. E. Granot, S. Sternklar, Y. Isbi, B. Malomed, and A. Lewis, "Sub-wavelength non-local spatial solitons," Opt. Commun. **166**, 121–126 (1999).
22. E. Granot, S. Sternklar, Y. Isbi, B. Malomed, and A. Lewis, "On the existence of subwavelength spatial solitons," Opt. Commun. **178**, 431–435 (2000).
23. B. V. Gisin and B. A. Malomed, "One- and two-dimensional subwavelength solitons in saturable media," J. Opt. Soc. Am. B **18**, 1356–1361 (2001).
24. N. N. Rosanov, V. E. Semenov, and N. V. Vyssotina, "'Optical needle' in media with saturating self-focusing nonlinearities," J. Opt. B **3**, S96–S98 (2001).